J. Fluid Mech. (1973), *vol.* 57, *part* 1, *pp.* 63–79
Printed in Great Britain

Natural convection in a sloping porous layer

By S. A. BORIES AND M. A. COMBARNOUS
Groupe d'Etude I.F.P.–I.M.F. sur les Milieux Poreux,
2 Rue Camichel, Toulouse, France

(Received 1 February 1972 and in revised form 26 June 1972)

This paper describes an experimental and theoretical study of thermal convection in a sloping porous layer. The saturated layer is bounded by two parallel impermeable planes maintained at different temperatures. Several types of flows were observed: a unicellular movement and a juxtaposition of longitudinal coils or of polyhedral cells.

A theoretical analysis has been made using the standard bases of the linear theory of stability and by taking into account some assumptions suggested by experimental observations. The critical conditions for the transition between unicellular and polycellular flows has been determined. For flow in longitudinal coils or with polyhedral cells the average heat transfer depends mainly on the filtration Rayleigh number and on the slope of the layer.

The experimental study was made in a Rayleigh number range 0–800 and for various slopes (0–90°). For both the transition criterion and the heat transfer, a good fit was observed between the experimental and theoretical results. For maximum slope, i.e. 90°, a correlation which connects the Nusselt number with both the Rayleigh number and the vertical extent of the model is proposed.

1. Introduction

Thermal convection in porous media is of great importance in numerous practical fields such as chemical engineering, geothermal activities and some oil recovery techniques. For the case of a homogeneous horizontal layer a number of studies have been published. This paper is devoted to a study of thermal convection in a sloping porous layer. The layer is bounded by two impermeable planes maintained at different temperatures and its lateral extent is quite large compared with its thickness. In this study, our attention has mainly been focused on theoretical and experimental approaches to both the convective flow organization and mean heat transfer.

From the phenomenological standpoint there is a fairly close analogy between convective motions in a porous medium and in a fluid layer. Concerning inclined fluid layers, some recent papers give theoretical and experimental information regarding the fluid motions (Hart 1971*a*, *b*; Unny 1972). Hart has observed two types of convective motions: a unicellular motion and a helical coil regime. As is indicated in the present paper, these types of flow have also been observed in a porous layer.

2. Thermal convection in porous media

In a porous medium the buoyancy force which causes convection may be put in a dimensionless form by the use of a filtration Rayleigh number Ra^* which is slightly different from the standard Rayleigh number defined in a fluid alone. For a porous layer bounded by equidistant isothermal surfaces this number is written as

$$Ra^* = g\frac{\alpha(\rho c)_f}{\nu}\frac{K}{\lambda^*}\Delta T H, \tag{1}$$

where g is the gravitational acceleration, α, $(\rho c)_f$ and ν are respectively the thermal expansion coefficient, the heat capacity and kinematic viscosity of the fluid, K is the permeability, λ^* the thermal conductivity of the porous medium saturated with the motionless fluid and ΔT the temperature difference between the two surfaces which are separated by a distance H.

The main consequence of convective motion is to increase the mean heat transfer. This can be expressed by a Nusselt number

$$Nu^* = \lambda_c/\lambda^* = \phi H/(\lambda^*\Delta T), \tag{2}$$

ϕ being the heat flow density due to both conduction and convection between isothermal planes, and λ_c the overall thermal conductivity coefficient of the layer when convection occurs.

The results available for the case of a *horizontal layer* mainly concern the convection criterion, the convective flow pattern and the mean heat transfer. They have been obtained using a linear theory, some variational techniques (Westbrook 1969), extensive experimentation and numerical computations.

The criterion for the onset of convection in a horizontal layer has been computed for different boundary conditions (Nield 1968) but theoretical and experimental work is mainly devoted to the case of impermeable isothermal boundaries. In this case the standard criterion for the onset of natural convection, i.e. $Ra^* \geqslant 4\pi^2$ (Horton & Rogers 1945; Lapwood 1948), is well confirmed by the experiments.

If Ra^* is higher than $4\pi^2$ but not too large, a stable convective state exists. It is characterized by adjacent polyhedral cells, which have been visualized for a layer with a free upper surface (Bories 1970*a*, *b*), see figure 1 (plate 1). The size of the convective cells may be described in dimensionless form and, for instance, if the convective motion looks like two-dimensional rolls, the reduced size of each roll E/H, where E is the width of the roll, is equal to one for Ra^* close to $4\pi^2$.

Another convective state has been found for Ra^* higher than a critical value which lies in the range 240–280 depending on the porous medium (Combarnous 1970*a*, *b*). This state, which is called the fluctuating convective state, corresponds to continuous creation and disappearance of convective cells, even in the thermal steady state (Caltagirone, Cloupeau & Combarnous 1971), see figure 2.

Concerning mean heat transfer due to convection, whereas a standard mathematical study leads, as for the case of a fluid layer, to a unique relationship between the Rayleigh and Nusselt numbers, experimental data (Schneider1963;

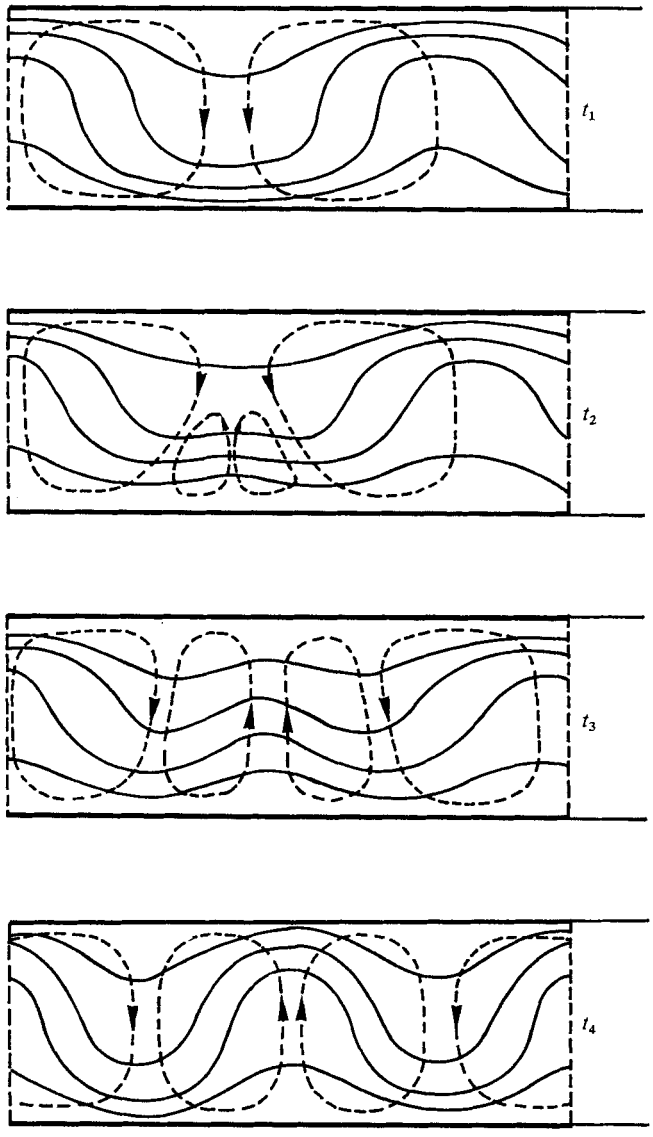

FIGURE 2. Experimental observation by the Christiansen effect of the evolution of two-dimensional convective rolls in a thermal steady state for the fluctuating convective state (Caltagirone, Cloupeau & Combarnous 1971). ($t_4 - t_1$ is about 1 hour.)

Combarnous 1970*a*) have shown that the mean heat transfer does not depend solely on the Rayleigh number but also on the thermal characteristics of the constituting phases, the solid matrix and the saturating fluid. This is probably due to the invalidity of the assumption of an infinite heat-transfer coefficient between fluid and solid phases, an assumption which is generally made in the mathematical formulation of the heat transfer (equation (5)).

In the case of a *sloping porous layer*, published studies are not very numerous. Excluding some numerical works (Holst 1970; Vlasuk 1972) and a partial experi-

mental investigation (Kaneko 1972) in a sloping box having all dimensions of the same order of magnitude, the only published results to our knowledge concern the vertical layer (Schneider 1963; Chan, Ivey & Barry 1970; Klarsfeld 1970).

3. Mathematical formulation

The saturated porous medium is contained in a rectangular model. ϕ is the angle of the layer with respect to the horizontal position and H, L and W are respectively the thickness, length and width of the model (figure 3). T_1 is the temperature of the upper plane and $T_2 = T_1 + \Delta T$ that of the lower plane. Lateral boundaries are rigid and insulating. Furthermore, in order to reduce the effect of lateral boundaries, the ratios L/H and W/H are much larger than 1.

With the assumptions and approximations which are frequently used for thermal convection in a homogeneous porous medium saturated with an incompressible fluid, the general equations may be written as (Wooding 1957):

$$\epsilon \partial\rho/\partial t + \operatorname{div}(\rho \mathbf{V}) = 0, \tag{3}$$

$$\frac{1}{\epsilon}\frac{\partial \mathbf{V}}{\partial t} = -\frac{1}{\rho}\operatorname{grad} p - \frac{\nu}{K}\mathbf{V} + \mathbf{g}, \tag{4}$$

with $$\mathbf{g} = (-g\sin\phi, 0, -g\cos\phi),$$

$$(\rho c)^* \partial T/\partial t = \lambda^* \operatorname{div}(\operatorname{grad} T) - \operatorname{div}[(\rho c)_F \mathbf{V}T], \tag{5}$$

$$\rho = \rho_m[1 - \alpha(T - T_m)], \tag{6}$$

where ϵ is the porosity of the porous medium, $\mathbf{V}$ the filtration velocity, T the temperature, p the pressure and ρ the fluid density. T_m is a reference temperature level at which the density equals ρ_m.

Dimensional analysis derived on the basis of the set of equations (3)–(6) leads to the following dimensionless quantities:

$$\epsilon, \quad \frac{H}{L}, \quad \frac{H}{W}, \quad \alpha\Delta T, \quad \frac{(\rho c)^*}{(\rho_c)_f}, \quad \frac{K}{H^2}, \quad \nu_m(\rho c)_f/\lambda^*, \phi, \quad Ra^*. \tag{7}$$

With the standard Boussinesq hypothesis and assuming $H/W \approx 0$ the thermal convection steady state may be described, for a given porous medium, through the consideration of only the numbers H/L, ϕ and Ra^*. Then all the dimensionless quantities characterizing thermal convection and especially mean heat transfer may be expressed in terms of these numbers, e.g.

$$Nu^* = f(Ra^*, H/L, \phi). \tag{8}$$

4. Description of experiments

Experiments were performed for wide ranges of Ra^* (0–800) and slopes (0–90°) in a cell containing a saturated porous medium and with following dimensions: $L = 66{\cdot}3$ cm, $W = 46{\cdot}3$ cm and $H = 5{\cdot}0$ cm. The isothermal boundaries at $z = 0$, H are formed by two metal plates maintained at constant temperatures, in a thermal steady state. The upper plate is water cooled to T_1 and the lower one is warmed by electric resistors. As long as the slope of the layer is not too high no difficulty is encountered in maintaining the lower boundary isothermal. However,

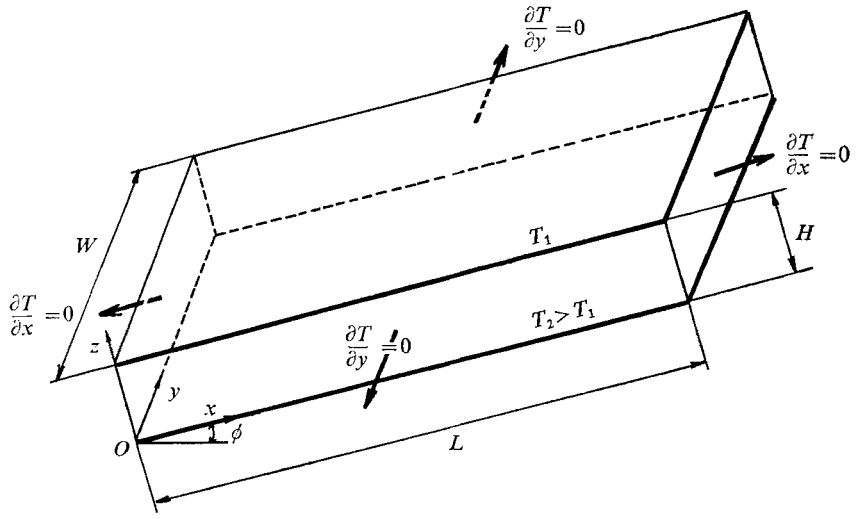

FIGURE 3. The porous layer.

for ϕ higher than 45°, a temperature gradient does appear along Ox during the experimental runs. This discrepancy from the ideal case is a maximum with a vertical layer: for instance, in this case, for Ra^* about 150, $\partial T_2/\partial x \approx 0{\cdot}12\,°\text{C/cm}$ with $\Delta T/H = 3{\cdot}5\,°\text{C/cm}$.

To ensure good insulation, the lateral sides of the model are made of plastic with a mean $\lambda \approx 0{\cdot}18\,\text{W/m}\,°\text{C}$ and a thickness of 6 cm. The lower part of the cell is carefully designed to prevent heat losses (mean λ of the insulation screen $\approx 0{\cdot}02\,\text{W/m}\,°\text{C}$).

The temperatures of the isothermal boundaries are measured by thermocouples set in grooves respectively at $x = \frac{1}{4}L$, $x = \frac{1}{2}L$ and $x = \frac{3}{4}L$. An intensive pattern of thermocouples is set in the porous medium so as to determine the convective currents: thermocouples may be translated along 14 horizontal lines 4 cm apart in the plane $z = \frac{1}{2}H$, in order to obtain continuous one-dimensional recordings.

With a uniform temperature equal to T_1 as the initial condition, a constant heat flow is dissipated in the lower plate, whose temperature T_2 is recorded versus time until the steady state is reached. The thermal conductivity λ^* due to conduction alone is measured both on the experimental cell with a downward heat flux and in a cylindrical thermal conductivity cell.

The porous media were made of spherical glass beads with diameters of 5·25, 4·7 and 3·25 millimetres. De-aerated water has been used as the saturating fluid. The permeability required for calculating Ra^* was computed from the Kozeny–Carman relationship.

5. Experimental observations on the organization of convective movements

Because of the mixture of approximations based on experimental results and other simplifying assumptions used in the analysis, in presenting this paper we shall divide the experimental results into two parts. The first, which is devoted

to the organization of convective movements, and concerns experiments performed in a Rayleigh number range 0–250, yields important results used as assumptions in the theoretical development. The second part, dealing with mean heat transfer, is presented after the theoretical analysis.

As is well known, in a vertical layer, when the Rayleigh number is not too high the convective motion is unicellular and two-dimensional. A hot upward current flows along the hot plate and the downward current goes down along the cold plate. In a sloping porous medium, for a Rayleigh number lower than a critical value Ra^*_ϕ, which depends on ϕ, the temperatures measured at $z = \frac{1}{2}H$ along lines parallel to Oy and not too close to the upper and lower boundaries of the experimental model are quite uniform; in addition, along these lines the temperature is independent of x (figure 4 (*a*)). This uniformity of the temperature for $z = \frac{1}{2}H$, in the central part of the model, has only been observed in a very homogeneous porous layer and indicates the existence of a unicellular unperturbed motion (figure 6 (*a*)).

When Ra^* is higher than Ra^*_ϕ the temperature distribution is not regular and several cases have to be distinguished.

(*a*) For ϕ lower than about 15°, the temperature distribution in the layer is analogous to that observed in a horizontal layer; i.e. the convective movements take the form of polyhedral cells. The limit $\phi = 15°$ is not very strictly defined; as was mentioned in §4, it has been observed for thermal steady states obtained with a uniform temperature distribution in the whole layer as the initial state for the experimental runs.

(*b*) For higher values of ϕ, temperature profiles recorded for $z = \frac{1}{2}H$ along lines parallel to Oy for several values of x ($x/L \in [0{\cdot}1\text{–}0{\cdot}9]$) are periodic, with the same wavelength and no phase shifting (figures 4 (*b*) and 5). Concerning the amplitudes, we observed that these are independent of x in the central zone of the model for $15° \lesssim \phi \lesssim 50°$ (figures 5 (*a*) and (*b*)). When ϕ increases, the influences, even in the central zone of the layer, of the non-uniformity of the temperature in the hot plate as well as of the end effects are not negligible and the amplitudes measured on the periodic temperature profiles are functions of x (figure 5 (*c*)).

(*c*) When the layer is quite vertical the convective motion tends to be unicellular. The ϕ value for transition between the periodic-temperature-profile state and the unicellular motion is strongly correlated with the extent L/H of the layer and we have observed periodic profiles, very smoothed by the influence of end effects, for ϕ up to 80°.

We may conclude from these observations that, for the slopes and Ra^* values (0–250) we have studied, convective movements take three different forms. For low values of Ra^* or for nearly vertical layers the movement is unicellular. For higher Ra^* values, (*a*) for low ϕ, the convective motions look like these observed in the horizontal layer and (*b*) for $\phi > \approx 15°$ a polycellular motion exists,

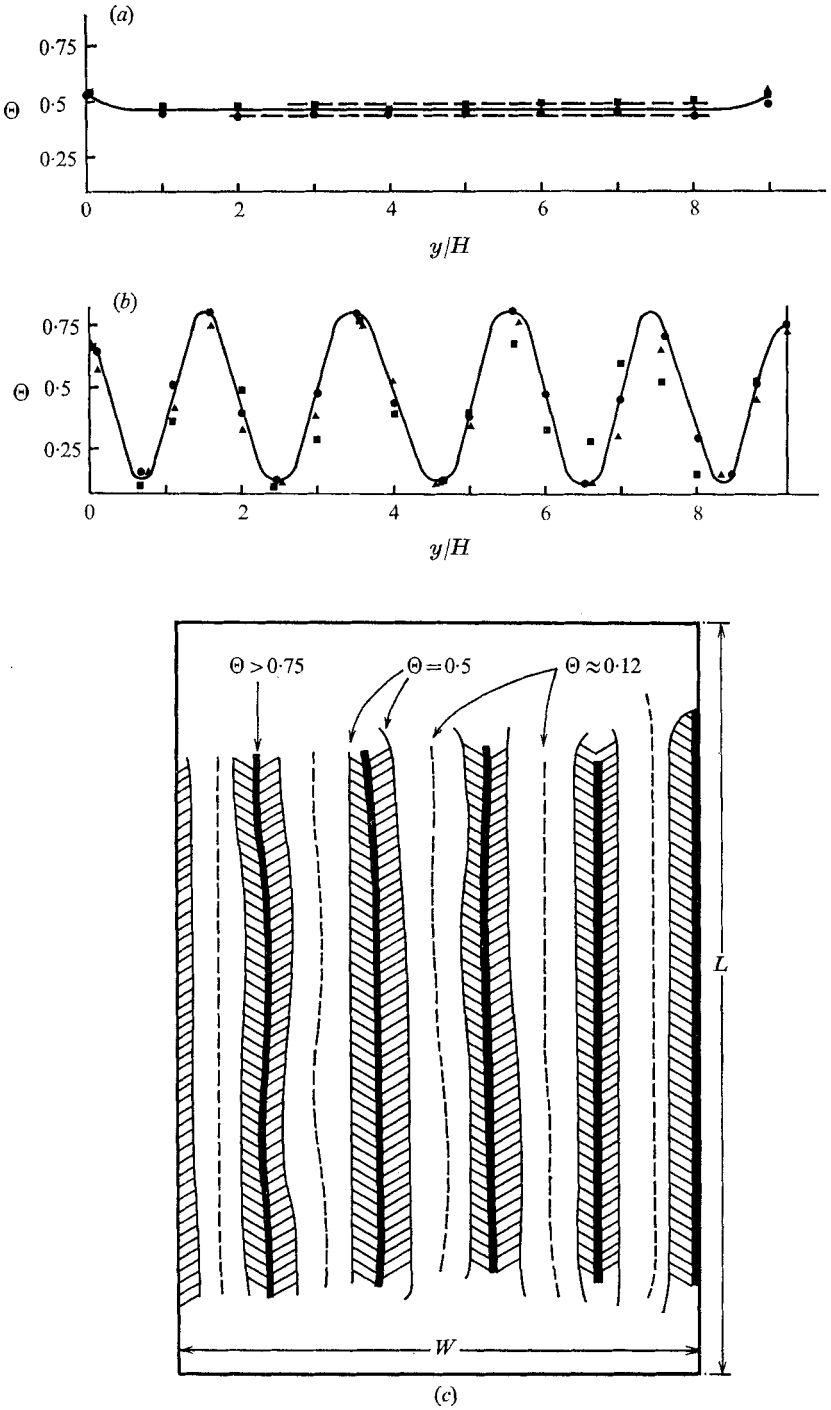

FIGURE 4. Temperature profiles measured on $z = \frac{1}{2}H$ along lines parallel to Oy for $\phi = 30°$ and (*a*) $Ra^* \cos\phi = 20 < 4\pi^2$ and (*b*) $Ra^* \cos\phi = 150 > 4\pi^2$. $\Theta \equiv (T - T_1)/(T_2 - T_1)$. ▲, $x/L = 0{\cdot}25$; ●, $x/L = 0{\cdot}50$; ■, $x/L = 0{\cdot}75$. (*c*) Map of temperature distribution in the layer for $z = \frac{1}{2}H$ with $\phi = 30°$ and $Ra^* \cos\phi = 150$.

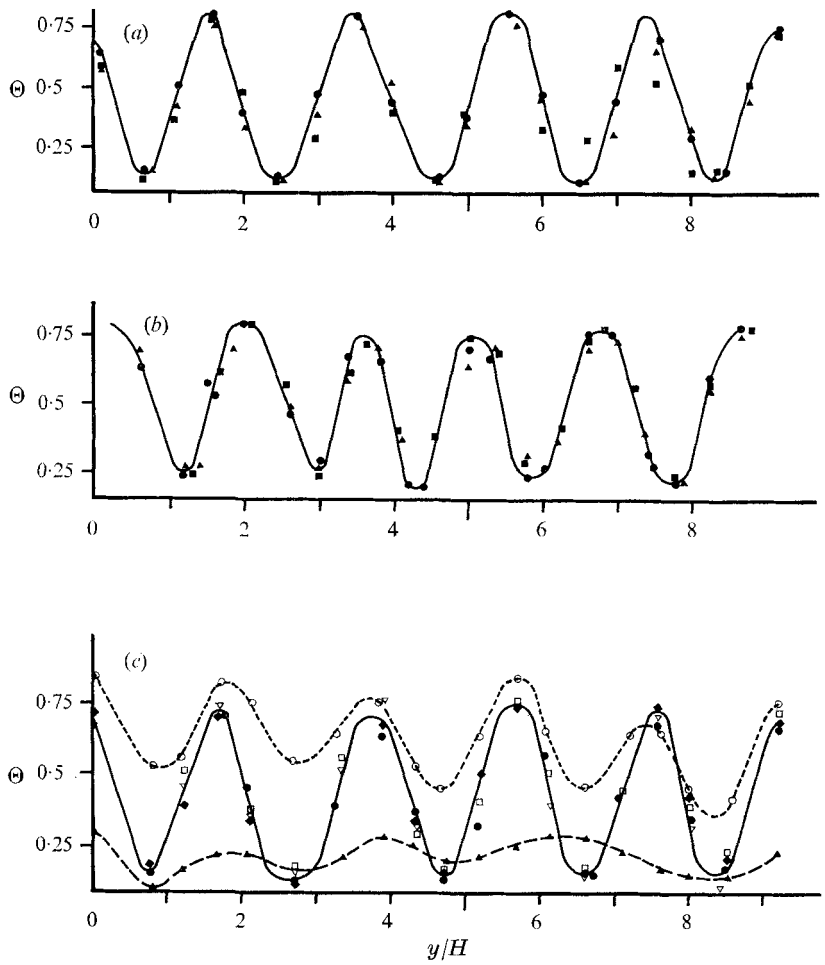

FIGURE 5. Temperature profiles measured on $z = \frac{1}{2}H$ along lines parallel to Oy for (a) $\phi = 30°$, $Ra^* \cos\phi \approx 120$, ($b$) $\phi = 45°$, $Ra^* \cos\phi \approx 150$ and (c) $\phi = 60°$, $Ra^* \cos\phi \approx 115$.

	▲	●	■	◆	▽	□	○
(a), (b) x/L	0·25	0·50	0·75	—	—	—	—
(c) x/L	0·15	0·40	—	0·47	0·51	0·58	0·82

and is characterized by adjacent coils climbing up along the slope direction (figure 6(b)). This motion is analogous to the one described by Hart in the fluid layer.

6. Theoretical description of the observations

This paragraph is mainly concerned with the longitudinal coil regime. For the study of both the criterion for the occurrence of this regime and mean heat transfer, we have analysed only the case of the infinite layer (H/L, $H/W = 0$). Concerning the comparison of this ideal case with the experimental conditions it must be emphasized that the existence of a solid matrix in the layer reduces the

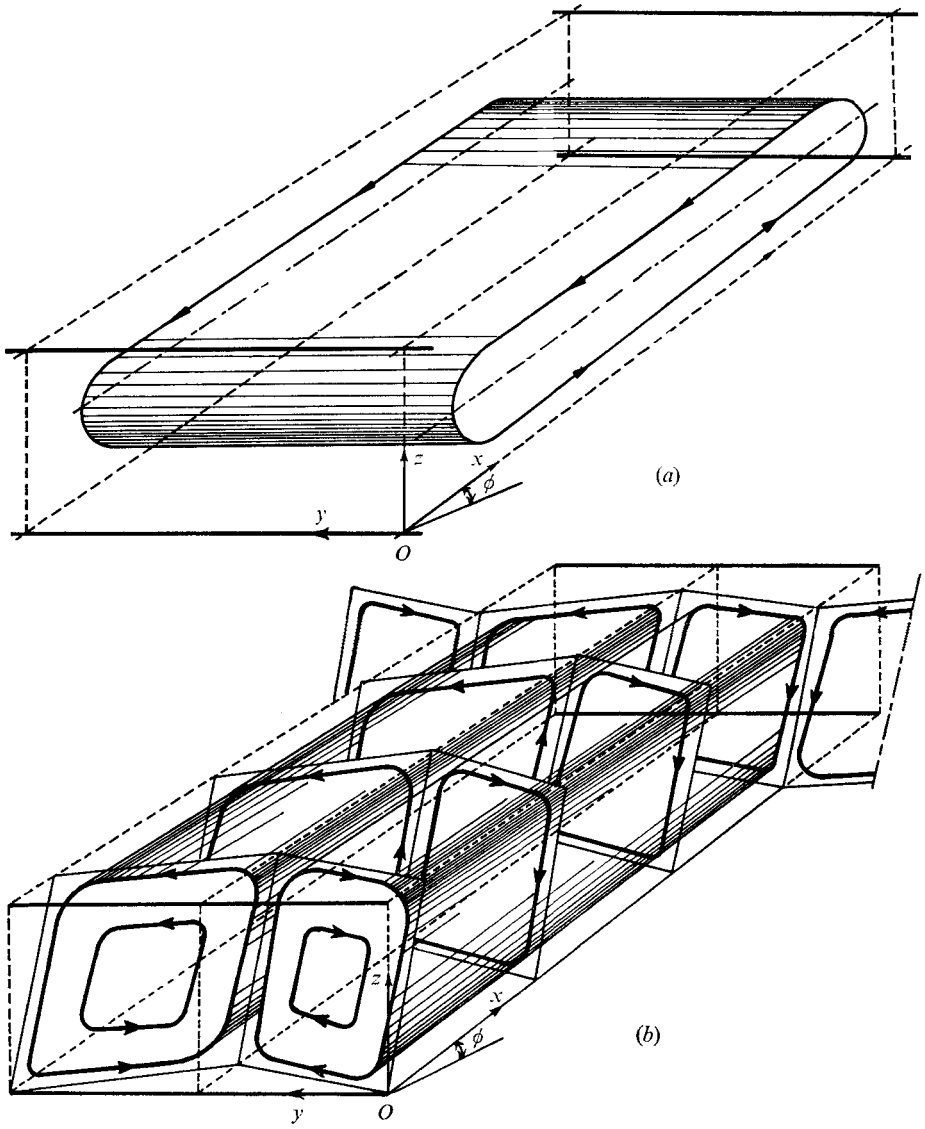

FIGURE 6. The two types of motion for $15° < \phi < 80°$: (*a*) the unicellular convective flow for $Ra^* \cos\phi < 4\pi^2$, (*b*) the longitudinal coil regime.

influence of the end effects on the flow pattern. So the values $H/L = 0{\cdot}075$ and $H/W = 0{\cdot}11$ of the experimental device, which might seem too large for a study in a fluid layer, are small enough in the case of a porous medium.

Unicellular motion

The unicellular motion is two-dimensional ($v_0 = 0$ and $\partial T/\partial y = 0$). In this case the equation set (3)–(6) is completed by the following boundary conditions:

$$\left.\begin{aligned} w_0 &= 0, \quad T = T_2 = T_1 + \Delta T \quad \text{for} \quad z = 0, \\ w_0 &= 0, \quad T = T_1 \quad \text{for} \quad z = H, \\ u_0 &= 0, \quad \partial T/\partial x = 0 \quad \text{for} \quad x = 0, L. \end{aligned}\right\} \tag{9}$$

The equation of motion and the energy equation yield

$$u_0 = -\frac{K}{\mu}\frac{\partial p}{\partial x} - \rho_m g \sin\phi\,[1-\alpha(T-T_m)], \tag{10}$$

$$w_0 = -\frac{K}{\mu}\frac{\partial p}{\partial z} - \rho_m g \cos\phi\,[1-\alpha(T-T_m)], \tag{11}$$

$$u_0\frac{\partial T}{\partial x} + w_0\frac{\partial T}{\partial z} = \frac{\lambda}{(\rho c)_f}\left(\frac{\partial^2 T}{\partial x^2} + \frac{\partial^2 T}{\partial z^2}\right), \tag{12}$$

with $T_m = \frac{1}{2}(T_1+T_2)$ and $\mu = \nu\rho$. In a section $x =$ constant, we may consider that

$$w_0 = 0, \quad \partial w_0/\partial z = 0. \tag{13}$$

Then from the continuity equation

$$\partial u_0/\partial x = 0, \quad u_0 = u_0(z). \tag{14}$$

However, from the experimental observations we know that $\partial T/\partial x \simeq 0$ (see figure 4). So the energy equation may be simplified to

$$\frac{\lambda}{(\rho c)_f}\frac{\partial^2 T}{\partial z^2} = 0. \tag{15}$$

As for a vertical porous layer, for low values of the Rayleigh number, the temperature profile along Oz is the same as the one resulting from pure conduction:

$$T = T_2 - \Delta T z/H. \tag{16}$$

By taking the derivatives of the equations of motion (10) and (11) with respect to z and x, we obtain

$$\frac{\partial^2 p}{\partial x\,\partial z} = -\frac{\mu}{K}\frac{\partial u_0(z)}{\partial z} - \rho_m g\alpha \sin\phi\frac{\Delta T}{H}, \tag{17}$$

$$\partial^2 p/\partial z\,\partial x = 0, \tag{18}$$

and hence $\partial u_0(z)/\partial z$. Then, as $u_0 = 0$ for $z = \frac{1}{2}H$.

$$u_0(z) = -\frac{K}{\mu}\rho_m g\alpha \sin\phi\frac{\Delta T}{H}\left[z - \frac{H}{2}\right]. \tag{19}$$

Longitudinal coils

The experimental study shows that, in a sloping layer with $15° \lesssim \phi \lesssim 80°$, when the Rayleigh number is increased the unicellular convective movement is replaced by a polycellular flow made up of a juxtaposition of longitudinal coils. Starting from the unicellular movement we look for the criterion for the onset of a polycellular movement using the standard linear theory approach. The coils are characterized by transverse perturbations from the unicellular movement.

Let $\mathbf{V}'$, p' and θ be the velocity, pressure and temperature perturbations from the initial movement defined by distributions $\mathbf{V}_0, p_0$ and T_0 which are solutions of (3)–(6). The variables in the new perturbed state, i.e.

$$\mathbf{V} = \mathbf{V}_0 + \mathbf{V}', \quad p = p_0 + p', \quad T = T_0 + \theta, \tag{20}$$

where $\mathbf{V} = (u_0+u', v_0+v', w_0+w')$, obey (3)–(6). If the Boussinesq assumption is taken into account the perturbation equation set is then

$$\frac{\partial u'}{\partial x}+\frac{\partial v'}{\partial y}+\frac{\partial w'}{\partial z} = 0, \tag{21}$$

$$\left(\frac{\rho_m}{\epsilon}\frac{\partial}{\partial t}+\frac{\mu}{K}\right)u' = -\frac{\partial p'}{\partial x}+\rho_m g\alpha(\sin\phi)\,\theta, \tag{22}$$

$$\left(\frac{\rho_m}{\epsilon}\frac{\partial}{\partial t}+\frac{\mu}{K}\right)v' = -\frac{\partial p'}{\partial y}, \tag{23}$$

$$\left(\frac{\rho_m}{\epsilon}\frac{\partial}{\partial t}+\frac{\mu}{K}\right)w' = -\frac{\partial p'}{\partial z}+\rho_m g\alpha(\cos\phi)\,\theta, \tag{24}$$

$$\frac{(\rho c)^*}{(\rho c)_f}\frac{\partial\theta}{\partial t}+u_0\frac{\partial\theta}{\partial x}+w'\frac{\partial T_0}{\partial z} = \frac{\lambda^*}{(\rho c)_f}\nabla^2\theta. \tag{25}$$

At this stage of the computation we use a simplifying assumption which is suggested by the experimental observations. Indeed, we have observed that in longitudinal-coil flow the temperature is uniform along any line parallel to Ox, i.e.

$$\partial\theta/\partial x = 0. \tag{26}$$

Then by using this assumption and eliminating w' and p' from (24) and (25) we obtain for the state of marginal stability ($\partial/\partial t = 0$)

$$\nabla^4\theta = \frac{K\rho_m g\alpha\Delta T}{\mu\chi H}\cos\phi\frac{\partial^2\theta}{\partial y^2} = \frac{Ra^*\cos\phi}{H^2}\frac{\partial^2\theta}{\partial y^2}, \tag{27}$$

with $\chi = \lambda^*/(\rho c)_f$. This equation differs from that for a horizontal layer by the existence of a multiplying factor $\cos\phi$.

We now look for a solution of (27) of the form

$$\theta = \theta(z)\,e^{ily}, \tag{28}$$

which is suggested by the experimental results. Then (27) is reduced to the dimensionless differential equation

$$(D^2-l^2)^2\theta = Ra^*\cos\phi\,l^2\theta, \tag{29}$$

with $D^2 = d^2/d\xi^2$ and $\xi = z/H$.

Hence we can find the function $\theta(z)$ by taking into account the boundary conditions. For the case we are concerned with here these conditions are

$$\theta = 0, \quad w' = (D^2-l^2)\,\theta = 0 \quad \text{for} \quad \xi = 0, 1.$$

Then we obtain the values of both the stability criterion and the perturbation wavelength. For instance, for the first mode of instability the criterion of existence is $Ra^*\cos\phi \geqslant 4\pi^2$ and the wavelength of perturbation $2\pi/l = 2H$.

The criterion for transition between the two flow regimes is then defined as

$$Ra^*\cos\phi = 4\pi^2. \tag{30}$$

This criterion, which we have derived only for the longitudinal-coil regime ($\partial T/\partial x = 0$), may be used for the occurrence of polyhedral convection, observed for $\phi < 15°$. In this case the assumption $\partial\theta/\partial x = 0$ is not valid but the term $u_0\partial\theta/\partial x$ in (25) is still negligible because of the small value of ϕ [equation (19)].

Considering (29), we also note that the only dimensionless quantity appearing in this equation is $Ra^* \cos\phi$. This shows that, for longitudinal-coil flow, all characteristic dimensionless quantities governing convection in a sloping porous layer of great extent depend solely on $Ra^* \cos\phi$, as long as the linear theory approximations are valid.

Relation between Nu^*, Ra^* and ϕ

In a horizontal porous layer, by using the Malkus power integral method, an analytical formulation of heat transfer has been developed (Aziz & Combarnous 1970; Bories 1970*a*, *b*) describing the Nusselt number as the sum of a series in which each term is associated with a different instability mode:

$$Nu = 1 + \sum_{n=1}^{\infty} k_n (1 - 4n^2\pi^2/Ra^*), \tag{31}$$

with

$$k_n = \begin{cases} 0 & \text{if} \quad Ra^* < 4n^2\pi^2, \\ 2 & \text{if} \quad Ra^* \geqslant 4n^2\pi^2. \end{cases}$$

The conclusion that we previously reached regarding the influence of the parameter $Ra^* \cos\phi$ induced us to look for a relationship similar to (31) for a sloping layer, in which Ra^* is replaced by $Ra^* \cos\phi$.

The Malkus technique starts with the integration, over the whole layer, of the energy equation and equations of motion with the terms of each equation multiplied respectively by the perturbations of the temperature and velocity distributions, θ and $\mathbf{V}'$. The integral relationships are then

$$\left(\beta - \frac{1}{\chi}\right) \int_0^H \langle \theta w' \rangle \, dz + \chi \int_0^H \langle \theta \nabla^2 \theta \rangle \, dz = \frac{1}{\chi H} \left[\int_0^H \langle \theta w' \rangle \, dz \right]^2, \tag{32}$$

$$\frac{\nu}{K} \int_0^H (\langle u'^2 \rangle + \langle v'^2 \rangle + \langle w'^2 \rangle) \, dz = g\alpha \sin\phi \int_0^H \langle \theta u' \rangle \, dz + g\alpha \cos\phi \int_0^H \langle \theta w' \rangle \, dz, \tag{33}$$

where the angled brackets indicate an average taken over planes parallel to the isothermal boundaries.

In order to proceed with the computation we need the values of the perturbation components. We know the θ distribution [equation (28)] and w' is computed from (25) and (26). Then the components of the curl of the equation of motion and the derivatives with respect to x and y of the continuity equation yield the values of u' and v':

$$u' = \frac{Kg\alpha}{\nu} \sin\phi \, \theta(z) \, e^{ily}, \tag{34}$$

$$v' = \frac{1}{l^2} \frac{\partial^2 w'}{\partial z \, \partial y}, \tag{35}$$

$$w' = \frac{2\lambda^* \pi^2}{(\rho c)_f \beta} \theta(z) \, e^{ily}. \tag{36}$$

With the value of u' inserted, (33) yields

$$\frac{\nu}{K} \int_0^H (\langle v'^2 \rangle + \langle w'^2 \rangle) \, dz = g\alpha \cos\phi \int_0^H \langle \theta w' \rangle \, dz. \tag{37}$$

As this equation is similar to the equation obtained in the case of a horizontal layer, with the exception of the multiplying factor $\cos\phi$ on the right-hand side, using the same procedure as in Catton (1966), we obtain

$$Nu^* = 1 + \sum_{n=1}^{\infty} k_n[1 - 4n^2\pi^2/(Ra^* \cos\phi)], \tag{38}$$

with

$$k_n = \begin{cases} 0 & \text{if} \quad Ra^* \cos\phi < 4n^2\pi^2, \\ 2 & \text{if} \quad Ra^* \cos\phi \geqslant 4n^2\pi^2. \end{cases}$$

This result leads to the following conclusion: the comparison between (31) and (38) shows that, for a given porous medium, a relation between Nu^* and $Ra^* \cos\phi$ is possible.

7. Experimental results on heat transfer

Sloping layer

The experimental heat-transfer results have been put in the form of a relation between Nu^* and $Ra^* \cos\phi$ (figure 7). These results concern experimental runs performed with a slope range 0–60° in a Rayleigh number range 0–800.

The correlation between Nu^* and $Ra^* \cos\phi$ values is quite good. For low values of Ra^* ($Ra^* \cos\phi < 4\pi^2$) the Nusselt number is greater than 1 because of the finite extent of the experimental model. However, for $Ra^* \cos\phi > 250$ a slight divergence is observed with the results obtained for slopes of 45° and 60°, and is probably due to both the end effects and the existence of a small temperature gradient in the hot plate.

On figure 7 we have also shown the theoretical relationship corresponding to equation (38); the discrepancy between experimental data and theoretical results is very important. We must recall that, as was mentioned in § 2, experimental information collected in the case of the horizontal porous layer indicates that the relationship between Nu^* and Ra^* depends on the characteristics of the porous medium. These two remarks emphasize the differences between thermal convection in porous media and in homogeneous fluid layers: indeed in the latter case there is no discrepancy between the whole set of experimental results and the theoretical relationship (Catton 1966).

The criterion for transition between the two types of flows which has been found seems to be well defined by relationship (30). This result can be compared with some experimental observations made in inclined fluid layers by Hart (1971*a*, *b*), see figure 8. Furthermore, the wavelength of the periodic temperature profiles observed (figures 4 and 5) corresponds to the theoretical wavelength of the perturbations, i.e. $2H$, for values of $Ra^* \cos\phi$ close to $4\pi^2$.

Vertical layer

We made some experiments on a vertical layer ($\phi = 90°$). As was previously mentioned, in the Rayleigh number range investigated, convective motion is unicellular. Some *in situ* temperature profiles with an appearance similar to those

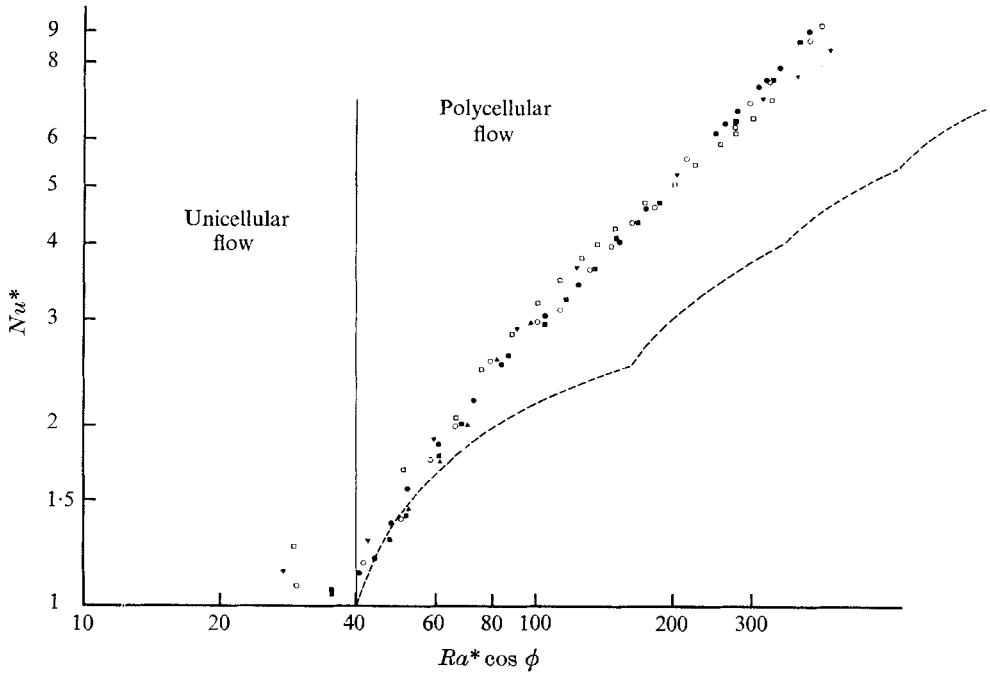

FIGURE 7. Mean heat-transfer results for the whole layer. Experimental data: ●, $\phi = 7{\cdot}5°$; ▲, $\phi = 15°$; ■, $\phi = 22{\cdot}5°$; ○, $\phi = 30°$; ▼, $\phi = 45°$; □, $\phi = 60°$; ———, theoretical relationship.

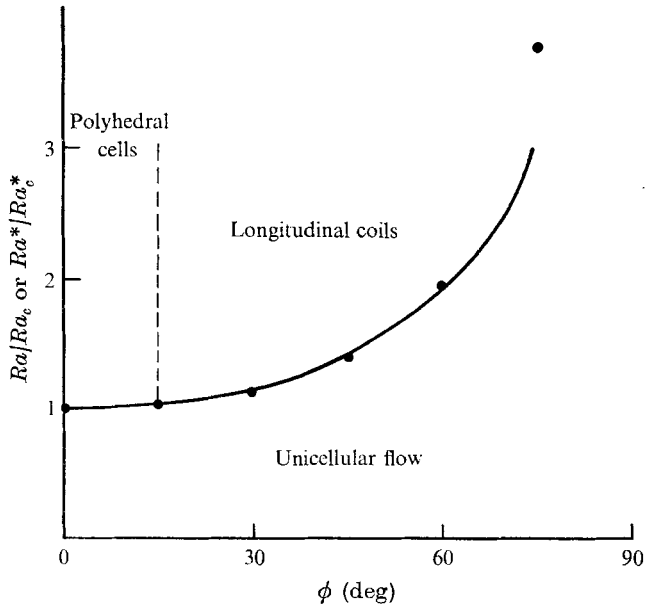

FIGURE 8. Criterion for transition between unicellular flow and polycellular flow. ———, fluid layer (Hart); ●, porous layer. $Ra_c^* \approx 40$; $Ra_c \approx 1708$.

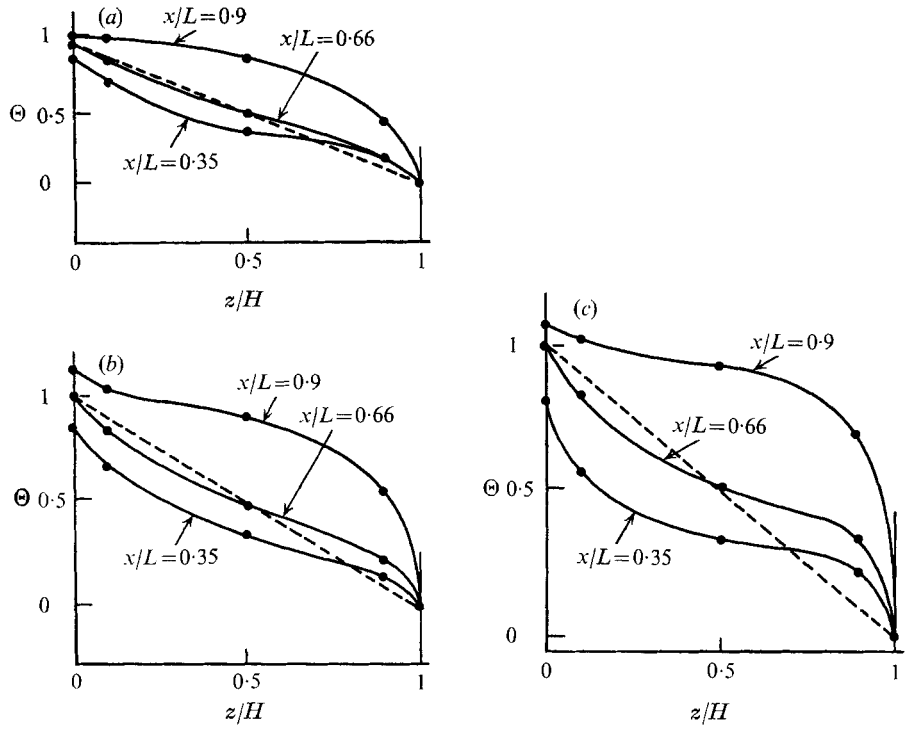

FIGURE 9. Temperature profiles in a vertical layer along lines parallel to Oz for various Ra^* values: (*a*) $Ra^* = 165$, (*b*) $Ra^* = 315$ and (*c*) $Ra^* = 520$.

computed by Holst (1970) or Chan *et al.* (1970) were recorded. Temperature profiles along horizontal lines corresponding to different x values show that for low values of the Rayleigh number (figure 9 (*a*)) the temperature profiles are not too different from these corresponding to the pure conduction state, except at the ends of the model. When the Rayleigh number increases we observe the development of thermal boundary layers along the plates. In this last case the centre of the model behaves like an isothermal zone (figure 9 (*c*)).

The heat-transfer results are very sensitive to the extent H/L of the model. A relation has been found between Nu^*, Ra^* and H/L:

$$Nu^* = 0{\cdot}245(Ra^*)^{0{\cdot}625}(H/L)^{0{\cdot}397}. \tag{39}$$

This relation includes our own results and the results published by Schneider (1963). It is valid for glass-bead porous media (ϵ about 0·38) saturated with water in a range of Ra^* from 10^2 to 10^3 and for values of H/L between 0·05 and 0·15. When $Ra^* = 100$, this relation can be compared with the numerical computations made by Chan *et al.* (1970) and Vlasuk (1972).

8. Conclusion

The theoretical and experimental results presented in this paper concern both the organization of the convective movements and the mean heat transfer due to convection in a sloping porous layer of large extent.

Two main results should be emphasized.

(i) Concerning the convective movements, two different types of flow have been observed in a sloping layer for $15° < \phi < 80°$. When $Ra^* \cos\phi < 40$ a unicellular two-dimensional movement takes place through the porous medium. When $Ra^* \cos\phi > 40$, convective movements are observed as a juxtaposition of longitudinal coils which are parallel to the slope of the layer.

(ii) Concerning the mean heat transfer, for a wide range of slopes (0–60°) and in the Rayleigh number range which has been investigated a unique relation between Nu^* and $Ra^* \cos\phi$ has been found.

This study has been done in the Groupe d'Etude I.F.P. – I.M.F. sur les Milieux Poreux, which is sponsored by the Institut Français du Pétrole in Rueil-Malmaison and the Institut de Mécanique des Fluides in Toulouse, which is an 'associated laboratory' to C.N.R.S. The authors wish to thank M. L. Monferran, who has been in charge of the experimental work, and M J. Y. Jaffrennou.

REFERENCES

Aziz, K. & Combarnous, M. A. 1970 Prédiction théorique du transfert de chaleur par convection naturelle dans une couche horizontale. *C.R. Acad. Sci.* B **271**, 813.

Aziz, K., Holst, P. H. & Karra, P. S. 1968 Natural convection in porous media. *19th Annual Meeting Petroleum Society C.I.M. (Calgary). Paper*, no. 6813.

Bories, S. A. 1970*a* Sur les mécanismes fondamentaux de la convection naturelle en milieu poreux. Ph.D. thesis, University of Toulouse.

Bories, S. A. 1970*b* Sur les mécanismes fondamentaux de la convection naturelle en milieu poreux. *Revue Gén. Therm.* **9** (108), 1377–1402.

Caltagirone, J. P., Cloupeau, M. & Combarnous, M. A. 1971 Convection naturelle fluctuante dans une couche poreuse horizontale. *C.R. Acad. Sci.* B **273**, 833–836.

Catton, I. 1966 Natural convection in horizontal liquid layers. *Phys. Fluids*, **9**, 2521–2522.

Chan, B. K. C., Ivey, C. M. & Barry, J. M. 1970 Natural convection in enclosed porous media with rectangular boundaries. *J. Heat Transfer*, **2**, 21–27.

Combarnous, M. A. 1970*a* Convection naturelle et convection mixte en mileu poreux. Ph.D. thesis, University of Paris.

Combarnous, M. A. 1970*b* Convection naturelle et mixte dans une couche poreuse horizontale. *Revue Gén. Therm.* **9** (108), 1355–1376.

Hart, J. E. 1971*a* Stability of the flow in differentially heated inclined box. *J. Fluid Mech.* **47**, 547–576.

Hart, J. E. 1971*b* Transition to a wavy vortex regime in convective flow between inclined plates. *J. Fluid Mech.* **48**, 265–271.

Holst, P. H. 1970 A theoretical and experimental investigation in porous media. Ph.D. thesis, University of Calgary.

Horton, C. W. & Rogers, F. T. 1945 Convection currents in a porous medium. *J. Appl. Phys.* **16**, 367–370.

Kaneko, T. 1972 An experimental investigation of natural convection in porous media. M.S. thesis. University of Calgary.

Katto, Y. & Masuoka, T. 1967 Criterion for onset of convective flow in a fluid in a porous medium. *Int. J. Heat Mass Transfer*, **10**, 297–309.

Klarsfeld, S. M. 1970 Champs de température associés aux mouvements de convection naturelle dans un milieu poreux limité. *Revue Gén. Therm.* **9** (108), 1403–1424.

Lapwood, E. R. 1948 Convection of a fluid in a porous medium. *Proc. Camb. Phil. Soc.* **44**, 508–521.

NIELD, D. A. 1968 Onset of thermohaline convection in a porous medium. *Wat. Resour. Res.* **4**, 353–360.

SCHNEIDER, K. J. 1963 Die Wärmeleitfähigkeit Körniger Stoffe und ihre Beeinflussung durch Freie Konvektion. Ph.D. thesis, Technischen Hochschule, Karlsruhe.

UNNY, T. E. 1972 Thermal instability in differential heated inclined fluid layers. *J. Appl. Mech.* **39**, 41–46.

VLASUK, M. P. 1972 Heat transfer with natural convection in permeable porous medium. IV*th All-Union Heat and Mass Transfer Conference* (*Minsk*), paper no. 1–49.

WESTBROOK, D. R. 1969 Stability of convective flow in a porous medium. *Phys. Fluids*, **12**, 1547–1551.

WOODING, R. A. 1957 Steady state free thermal convection of liquid in a saturated permeable medium. *J. Fluid Mech.* **2**, 273–285.

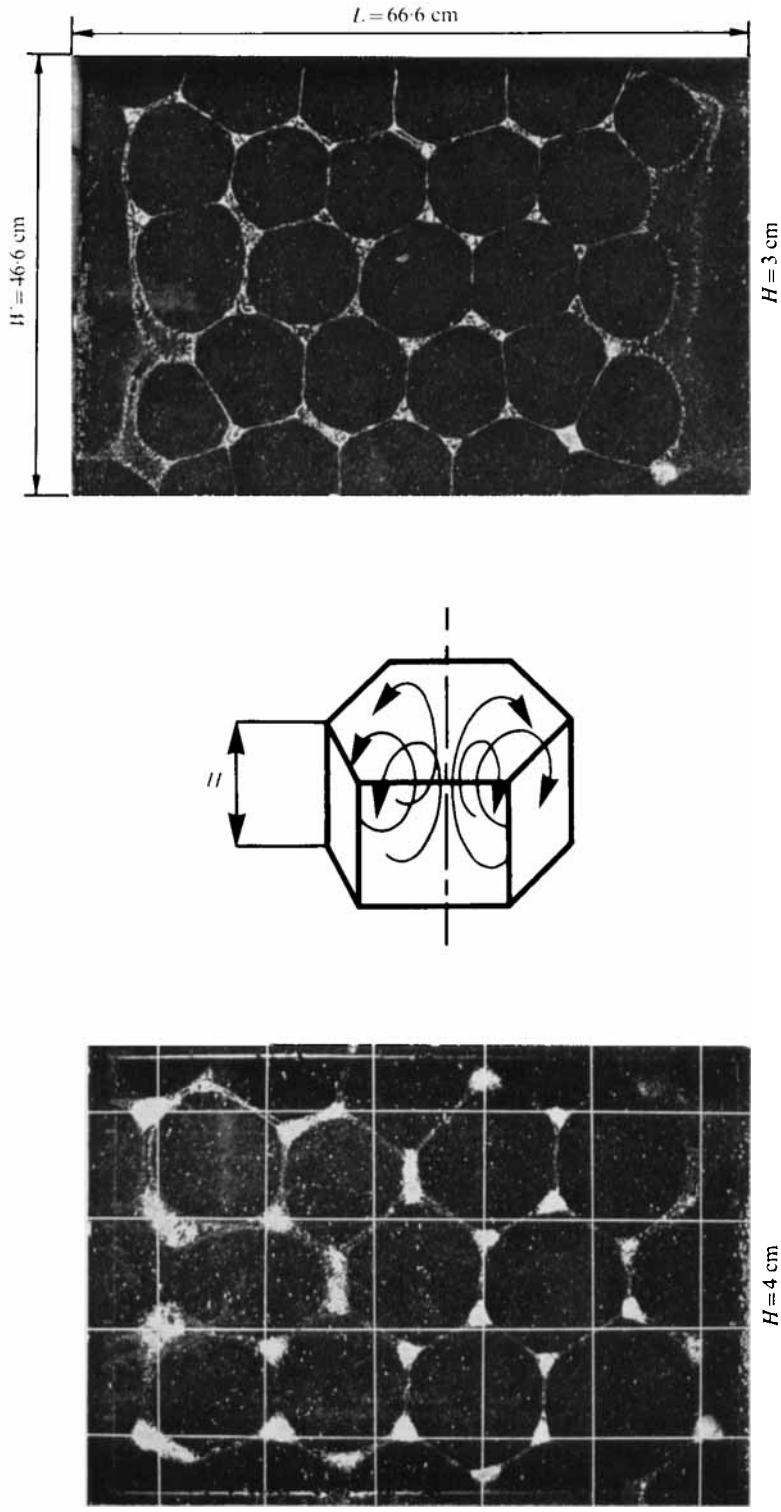

FIGURE 1. Convective polyhedral cells in a horizontal porous layer with a free upper boundary (Bories 1970*a*, *b*).